NEUROSCIENCE
RESEARCH ARTICLE
S. R. John et al. / Neuroscience 493 (2022) 69–80

Distinct Dynamics of Theta and Gamma Rhythmicity during Social Interaction Suggest Differential Mode of Action in the Medial Amygdala of Sprague Dawley Rats and C57BL/6J Mice

Shanah Rachel John, Wael Dagash, Alok Nath Mohapatra, Shai Netser and Shlomo Wagner*

Sagol Department of Neurobiology, Faculty of Natural Sciences, University of Haifa, Haifa 3498838, Israel

Abstract—The medial nucleus of the amygdala (MeA) is known to regulate social behavior. This brain area is functionally positioned in a crossroads between sensory information processing and behavioral modulation. On the one hand, it receives direct chemosensory input from the accessory olfactory bulb. On the other hand, it orchestrates various behavioral outputs via brain-wide projections under the regulation of multiple neuromodulatory systems. Previously, we showed that adult male Sprague Dawley (SD) rats and C57BL/6J mice, the most widely used rodent models in neuroscience research, differ in their dynamics of motivation to interact with a novel same-sex conspecific and that this difference correlates with the level of c-Fos expression in the MeA. Here we used chronically implanted electrodes to compare rhythmic local field potential signals recorded from these animals during free and restricted social interactions. We found a significant induction of rhythmicity in the theta (4–12 Hz) and gamma (30–80 Hz) bands during both free and restricted social interaction in both rats and mice. However, the induction of gamma rhythmicity, thought to reflect activity of local neuronal networks, was significantly higher in rats than mice. Nevertheless, in contrast to rats, mice exhibited induction of rhythmicity, in both the theta and gamma bands, in synchrony with investigation of social, but not object stimuli. These results suggest that during interaction with a novel same-sex conspecific, the MeA of C57BL/6J mice is mostly involved in sensory information processing while in SD rats it is mainly active in modulating the social motivation state of the animal.

Key words: medial amygdala, social interaction, *in vivo* recordings, electrophysiology, theta rhythmicity, gamma rhythmicity.

INTRODUCTION

The amygdala comprises multiple sub-nuclei (LeDoux, 2007; Sah et al., 2003), many of which regulate emotional and social behaviors (Allsop et al., 2018; Gadziola et al., 2012; Gangopadhyay et al., 2021; Huang et al., 2020; Kwon et al., 2021; Opendak et al., 2021; Twining et al., 2017). The medial nucleus of the amygdala (MeA) is known to be pivotal to various types of social behavior, including aggression, parenting, mating, and social recognition (Haller, 2018; Kohl et al., 2017; Newman, 1999; Petrulis, 2013; Walum and Young, 2018). Interestingly, this nucleus seems to be functionally positioned in a crossroads between sensory information processing and behavioral modulation (Raam and Hong, 2021). On the one hand, it receives direct and powerful chemosensory input from the accessory olfactory bulb that process all sensory signals arriving from the vomeronasal organ (Dulac and Wagner, 2006; Kohl et al., 2017; Martinez-Marcos, 2009; Mucignat-Caretta, 2010). On the other hand, it was shown to orchestrate various behavioral outputs via multiple brain-wide projections (recently reviewed by Raam and Hong, 2021). Moreover, the remarkably diverse convergence of neuromodulatory systems on this region suggest its involvement in shaping social behavior according to the animal's motivational state (Arakawa et al., 2010; Cushing et al., 2008; Frankiensztajn et al., 2018; Kwon et al., 2021; Shemesh et al., 2016; Stephens and Kauffman, 2017; Unger et al., 2015). Thus, the balance between the MeA role in sensory information processing and its role in behavioral modulation, a balance which may be species specific, is yet to be determined.

We previously reported that Sprague Dawley (SD) rats exhibit higher and more immediate motivation for interaction with a novel conspecific, as compared to C57BL/6J mice. Accordingly, we observed increased c-Fos expression in both the nucleus accumbens (NAc) and MeA of adult SD rats, already following two minutes of interaction with a novel conspecific, while C57BL/6J mice required a longer period of social interaction for

*Corresponding author.
E-mail address: shlomow@research.Haifa.ac.il (S. Wagner).
Abbreviations: LFP, local field potential; MeA, medial nucleus of the amygdala; NAc, nucleus accumbens; SD, Sprague Dawley; RDI, Relative differential investigation.

https://doi.org/10.1016/j.neuroscience.2022.04.020
0306-4522/

significant elevation of MeA c-Fos expression (Netser et al., 2020). Whereas the role of the NAc in regulating social motivation is relatively studied (Amadei et al., 2017; Dolen et al., 2013; Park et al., 2021; Walsh et al., 2018; Williams et al., 2020), this is not the case for the MeA. Nevertheless, several recent studies suggest that the MeA is involved in rewarding social activities such as social play in rats (Argue et al., 2017; Dumais et al., 2016; van Kerkhof et al., 2014), social reinforcement behavior in mice (Hu et al., 2021), and mother-infant bonding in humans (Atzil et al., 2017).

Previous studies by others (Bergan et al., 2014; Chen et al., 2019; Li et al., 2017; Yao et al., 2017a) and ourselves (Frankiensztajn et al., 2018; Tendler and Wagner, 2015) have attempted to gain insight into the neuronal mechanisms underlying the role of the MeA in social behavior and motivation. One of these mechanisms is neuronal synchrony. Neurons synchronize their activity to collective network rhythms, reflected by local field potential (LFP) signals, that serve to transfer information among distributed neuronal assemblies (Buzsaki and Draguhn, 2004; Uhlhaas et al., 2009). Indeed, such rhythms provide temporal windows for adequate communication between coordinated brain areas by allowing information processing at both neuronal and behavioral levels (Cannon et al., 2014; Li and Zhou, 2011; Wang, 2010). The most studied LFP rhythms are theta (4–12 Hz) and gamma (30–80 Hz) rhythms, which are thought to reflect different aspects of neuronal synchrony. While theta rhythmicity is assumed to reflect synchrony within distributed networks (Fujisawa and Buzsaki, 2011), gamma rhythmicity is considered to reflect synchrony in local networks (Buzsaki and Wang, 2012). Accordingly, theta rhythmicity is associated with extended brain states, such as attention and arousal, while gamma rhythmicity is thought to be briefly induced by arrival of specific inputs (Buzsaki and Watson, 2012; Jutras and Buffalo, 2010; Lisman, 2005).

In a previous study, we demonstrated the induction of theta rhythmicity in a network of limbic brain areas, including the MeA, during social interaction between adult male SD rats. Since the power of theta rhythmicity depended on familiarity between the animals, we suggested that theta rhythmicity in the MeA and other limbic regions reflects the social motivational state of the animal (Tendler and Wagner, 2015). In the current study we aimed to examine neural correlates in the MeA in SD rats and C57BL/6J mice to social interactions with novel social stimuli in a controlled environment. For this purpose, we used a controlled setting of social interaction, that enables precise analysis of the temporal change in theta and gamma rhythms, via *in vivo* extracellular recordings, in relation to specific behavioral events.

EXPERIMENTAL PROCEDURES

Animals

All animals were kept in the animal facility of the University of Haifa under veterinary supervision, in a 12 h light/12 h dark cycle (lights on at 9 PM), with *ad libitum* access to food (standard chow diet, Envigo RMS, Israel) and water. Mouse subjects (n = 8) were naïve C57BL/6J adult male mice (10–15 weeks old), commercially obtained (Envigo, Israel) and housed in groups of 2–5 per cage. Mouse stimuli were in-house grown C57BL/6J juvenile male mice (3–6 weeks old). Rat subjects (n = 7) were Sprague Dawley (SD) male rats (9–15 weeks old) grown in-house and kept in groups of 2–5 animals per cage. Rat stimuli were in-house grown SD juvenile male rats (5–6 weeks old). Prior to the electrode implantation surgery, rats were handled daily for 1–2 weeks. After implantation, both rats and mice were kept in isolation for about 7 days. Behavioral experiments took place during the dark phase of the diurnal cycle, under dim red light. All experiments were performed according to the National Institutes of Health guide for the care and use of laboratory animals, and approved by the Institutional Animal Care and Use Committee of the University of Haifa.

Experimental setups

The experimental setups were as previously described (Netser et al., 2019). Briefly, the mouse setup consisted of a white Plexiglas arena (37 × 22 × 35 cm) placed in the middle of an acoustic chamber (60 × 65 × 80 cm). Two Plexiglas triangular chambers (12 cm isosceles, 35 cm height) were placed in two randomly selected opposite corners of the arena, in which an animal or object (plastic toy) stimulus could be placed. A metal mesh (12 × 6 cm, 1 × 1 cm holes) placed at the bottom of the triangular chamber allowed direct interaction with the stimulus through the mesh. A high-quality monochromatic camera (Flea3 USB3, Point Grey), equipped with a wide-angle lens, was placed at the top of the acoustic chamber and connected to a computer, enabling a clear view and recording (30 frames/s) of the subject's behavior using a commercial software (FlyCapture2, Point Grey).

The rat setup was similar to the mouse setup, with different dimensions and colors in order to fit them to the size and color of SD rats. A black matte Plexiglas arena (50 × 50 × 40 cm) was placed in the middle of an acoustic chamber (90 × 60 × 85 cm). Inside the arena, two black Plexiglas triangular chambers (20.5 cm isosceles, 40 cm height) were placed in two randomly selected corners, with a metal mesh (25 × 7 cm, 2.5 × 1 cm holes) covering the bottom of the triangular chamber. The video system was as described for mice.

Behavioral paradigms

The behavioral paradigm started with a 15-min habituation to the arena with empty chambers. Throughout this time, social stimuli were placed in other chambers for acclimation. The recording session started with an additional 5 min of baseline with the empty chambers. Thereafter, the empty chambers were replaced with the social and object (plastic toy, ~5 × 5 cm) stimuli chambers, and the restricted interaction test was performed for 5 min. Following the restricted

interaction test, the chambers with the stimuli were removed from the arena, and the subject was left alone for 15 min. Next, the recording started again for an additional 5 min of baseline followed by a 5-min test of free interaction with a novel social stimulus (see Fig. 1A for a schematic description of the paradigm). Each subject animal was tested 2–3 times, with at least 24 h separating between distinct session with the same subject.

Tracking software

All recorded video clips were analyzed using TrackRodent (https://github.com/shainetser/TrackRodent) as previously described (Netser et al., 2019). For analysis of restricted interaction sessions, we used the *BlackMouseWiredBodyBased* and *WhiteRatWiredHeadDirectBased* algorithms and for free interaction sessions we employed the *BlackMice_TwoMiceFreeInteraction* and

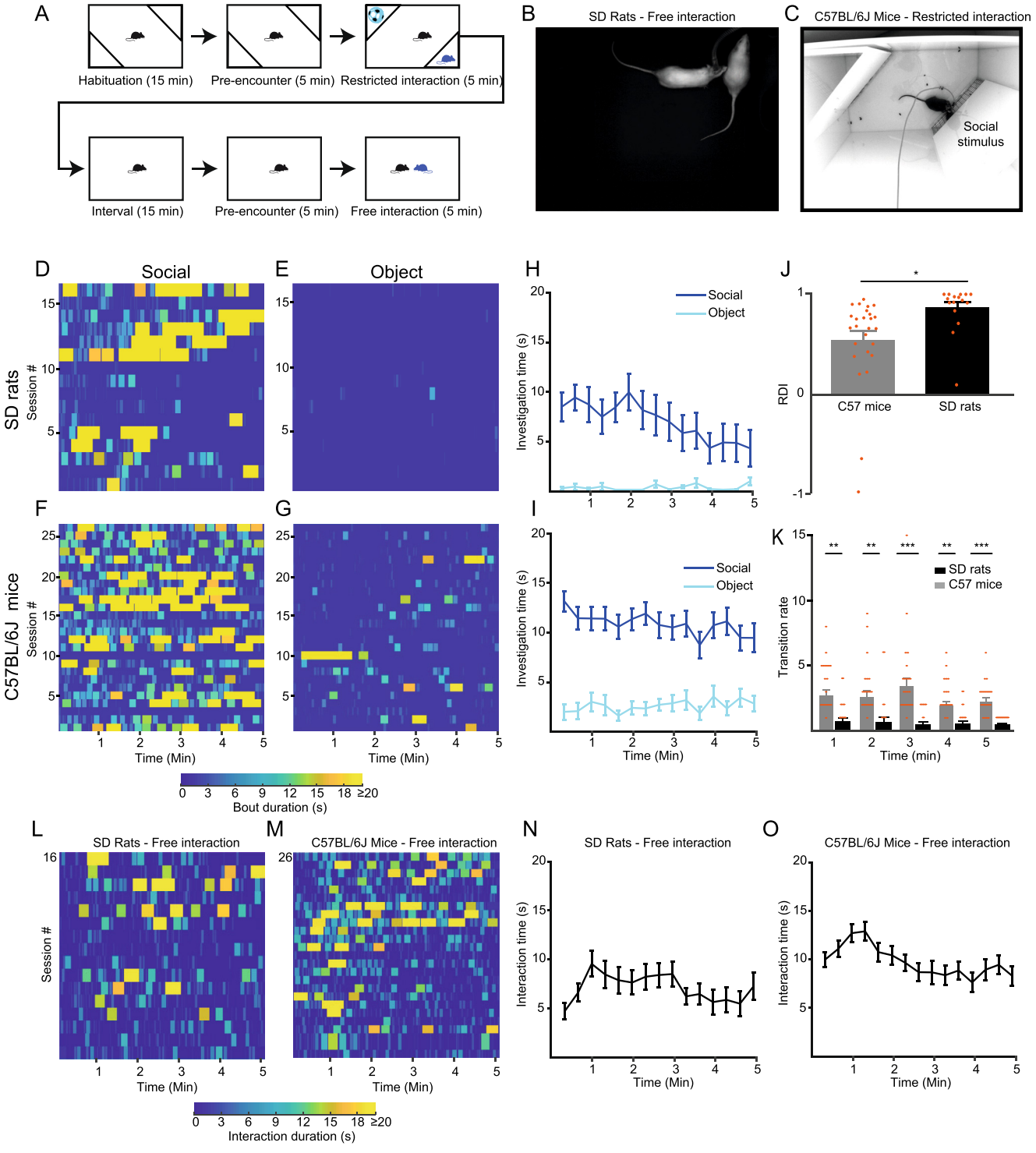

WhiteRats_TwoRatsFreeInteraction algorithms. The latter two algorithms use the body contours of both animals to define video frames in which the two animals touch one another. These frames were defined as social interaction, regardless of the nature of the interaction.

Behavioral analyses

Behavioral analysis was carried out as previously described in detail (Netser et al., 2019). Investigation time was calculated in 20 s bins across a 5-min test session. Relative differential investigation (RDI) was defined as the absolute value of the difference in investigation time between the two stimuli, divided by their sum. A transition between stimuli was defined as the time point when investigation of a new stimulus (relative to the other stimulus) started. The mean rate of transitions was calculated at 1 minute bins.

Electrophysiology

Electrode implantation surgery. Rats and mice were anesthetized with an intraperitoneal injection of a mixture of ketamine and Domitor [rats: 0.09 mg/gr and 0.0055 mg/gr, respectively; mice: 0.13 mg/gr and 0.01 mg/gr, respectively], and the painkiller Norocarp [rats: 0.016 mg/gr; mice: 0.005 mg/gr]. Anesthesia level was monitored by testing toe pinch reflexes. The body temperature of the animals was kept constant at approximately 37 °C, using a closed-loop custom-made temperature controller connected to a temperature probe and a heating pad placed under the animal. Anesthetized animals were fixed in a stereotaxic apparatus (rats: Stoelting Inst.; mice: Kopf Inst.), with the head flat. The skin was then gently removed, and holes were drilled in the skull for implantation of a single wire electrode (50 μm tungsten wire, California Fine Wires – California, US; 30-150kΩ), connected to a Mill-Max connector glued to a custom-made 3D plastic-printed scaffold in the MeA (rats: A/P = −2.40 mm, L/M = −3.18 mm, D/V = −8.50 mm; mice: A/P = −1.70 m m, L/M = −2.00 mm, D/V = −5.00 mm), and for reference/ground (100 μm silver wire, AM systems) and screw connections. Before implantation, electrodes were coated with a dye, DiI (1,1′-Dioctadecyl-3,3,3′,3′-tetrame thylindocarbocyanine perchlorate, dissolved in 70% ethyl-alcohol; Invitrogen), for fluorescent marking aimed to track their position postmortem. Implanted electrodes were fixed by dental cement. Following surgery, animals received daily injections of painkiller for three days and were allowed to recover for at least five days before experiments.

Electrophysiological recordings. All experiments were conducted in experimental arenas as described above for the behavioral experiments. Electrophysiological recordings were performed via the RHD2000 evaluation system, using an ultra-thin SPI interface cable and a RHD2132 amplifier board (Intan Technologies). A custom-made Omnetics-to-MillMax adaptor was used to connect between the electrode and amplifier. Recorded signals (sampled at 20 kHz) were synchronized with the video recording by a start signal sent through a custom-made triggering device and TTL signals from the camera to the recording system.

Analysis of LFP signals. All signals were analyzed using a custom-made MATLAB program. First, the signals were down-sampled to 5000 Hz and low-pass filtered up to 300 Hz using a Butterworth filter. The power over time for the different frequencies was constructed by the ‘‘spectrogram” function in MATLAB, using a 2 s long discrete prolate spheroidal sequences (DPSS) window with 50% overlap, at 0.5 Hz increments and 0.5 s time bins. The power for each frequency band (Theta: 4–12 Hz and Gamma: 30–80 Hz) was averaged, and the delta in dB was calculated relative to the mean power averaged across the entire 5 min of pre-exposure (Baseline) period. For presentation purposes, the average delta of the power (Δpower) was calculated in 10 s bins.

Synchronization between LFP signal and investigation bouts towards social or object stimuli was assessed by calculating the gamma power within a time window of 5 s before and 5 s after the beginning of each bout (using 1 s bins) and then averaging all bouts for each session.

Fig. 1. SD rats display higher levels of social preference than C57BL/6J mice. (**A**) A scheme depicting the various stages of the social interaction behavioral paradigm. (**B**) A picture from above of two SD rats during free social interaction. (**C**) A picture from above of a C57BL/6J mouse subject during restricted interaction with a social stimulus. (**D**) A heat-map of the investigation bouts conducted by SD rats towards the social stimulus across the 5-min restricted interaction session, color-coded according to bout duration (see color-code on the right). Each line represents a single session. (**E**) As in **(D)**, for the object stimulus during the same sessions. (**F**) As in **(D)**, for C57BL/6J mice. (**G**) As in **(F)**, for the object stimulus during the same sessions. Note the almost complete absence of investigation bouts towards the object in rats **(E)**, as compared to mice **(G)**. (**H**) Mean (± SEM, averaged across sessions) investigation time of SD rats, calculated separately for each stimulus across the restriction interaction session, using 20 s bins. (**I**) As in **(H)**, for C57BL/6J mice. (**J**) A comparison between rats and mice of relative differential investigation (RDI) between the social and object stimuli. $*p < 0.05$, 2-tailed *t*-test. (**K**) A comparison between rats and mice in the rate of subject transitions between the two stimuli, calculated separately for each of the five minutes of the session. Note that mice displayed a significantly higher rate of transitions than rats throughout the session. $**p < 0.01$, $***p < 0.001$, Holm–Sidak's *post hoc* test following main effect in repeated ANOVA test. (**L**) A heat-map of the investigation bouts conducted by SD rat subjects towards the social stimulus across the 5-min free interaction session, color-coded according to bout duration (see color-code below). Each line represents a single session. (**M**) As in **(L)**, for C57BL/6J mice. (**N**) Mean (± SEM, averaged across sessions) interaction time of SD rat sessions shown in **(L)**, across the free interaction sessions using 20 s bins. (**O**) As in **(N)**, for C57BL/6J mouse free interaction sessions shown in **(M)**. (For interpretation of the references to colour in this figure legend, the reader is referred to the web version of this article.)

Thereafter, the mean gamma power was normalized separately for each session using *Z*-score analysis, with the 5 s before the bouts serving as baseline.

Histology and electrode registration

Animals were perfused with phosphate buffer saline (PBS) and then fixed using 4% paraformaldehyde (PFA) solution. The brains were harvested and placed in PFA (4%) for 48 h, followed by sectioning of 50-μm slices in the horizontal axis using a VT1000s Leica sliding vibratome. Sections were stained with DAPI and examined under a wide-field fluorescence microscope (Nikon Ti-eclipse) for verifying the placement of the electrode marks (DiI fluorescence) within the MeA (Fig. S1).

Statistical analysis

All averaged data are shown as mean ± SEM values. Statistical tests were performed using GraphPad Prism 7.04 or MATLAB (statistical toolbox 2021a). Normal distribution of the data was tested using the Kolmogorov–Smirnov and Shapiro–Wilk tests. A paired t test was used to compare between different conditions or stimuli for the same single group, and a student's t test was used to compare a single parameter between distinct groups. For comparison between multiple groups and parameters, an analysis of variance (ANOVA) test was applied to the data. All ANOVA tests were followed, if main effect or interaction was found, by *post hoc* Holm–Sidak's multiple comparison test corrections. Significance was set at 0.05 and was adjusted when multiple comparisons were used.

RESULTS

To record electrophysiological activity from the MeA of behaving rats and mice, we chronically implanted wire electrodes in the MeA of SD rats (n = 7, 16 sessions) and C56BL/6J mice (n = 8, 25 sessions). Following recovery from surgery, we recorded local field potential (LFP) signals before and during interactions with a social stimulus of the same sex and age, which was either located within a chamber (restricted interaction) or freely moving in the arena (free interaction). Each recording session, which followed a 15-min habituation period, comprised a 5-min Baseline stage in the absence of social or object stimuli and a 5-min Encounter stage (restricted or free interaction; Fig. 1A–C). For restricted interaction sessions, we automatically detected all the events where the subject investigated each of the stimuli in the chambers (social or object stimulus) using the TrackRodent system, as previously described by us (Netser et al., 2019). We then analyzed the time dedicated by the subject to investigating the stimulus-containing chamber (investigation time) along the time course of the session, separately for each stimulus. As apparent in Fig. 1D–I, both rats (Fig. 1D, E, H) and mice (Fig. 1F, G, I) showed significantly higher preference to investigating the social stimulus over the object throughout the restricted interaction. As previously described by us (Netser et al., 2020), rats exhibited almost no interest in investigating the object (Fig. 1E) as opposed to mice (Fig. 1G). This difference between the groups is also apparent from the relative investigation duration (RDI) index, which showed significantly higher values for rats as compared to mice (independent t-test; t = 2.608, df = 40, p = 0.013; Fig. 1J). Moreover, mice showed higher levels of transitions between the stimuli throughout the session (Mixed-model ANOVA, species – $F_{1,40}$ = 33.18, p < 0.001; time – $F_{2.822,112.9}$ = 1.168, p = 0.323; species × time – $F_{4,160}$ = 1.212, p = 0.308; Fig. 1K), suggesting a lower level of social preference. Nonetheless, the electrophysiologically recorded rats did not show higher social interaction time compared to mice, in contrast to our results with untethered animals (Netser et al., 2020). Similar results were obtained in the free interactions, where we automatically analyzed the periods of direct interactions between the animals (Fig. 1L–O).

In order to examine the electrophysiological correlates of our behavioral findings, rhythmicity of LFP signals was quantified using power spectral density analysis (Fig. 2A–D) separately for the theta (4–12 Hz) and gamma (30–80 Hz) rhythms. We first analyzed the changes in theta and gamma power of the LFP signals that are generally induced by the condition of social interaction by calculating the power along the time course of each session using 10 s bins. We then subtracted the mean power averaged across the 5-min Baseline stage from all bins, to calculate the change in power (ΔPower) separately for each rhythm (theta and gamma). Both rats and mice showed significant increase of ΔPower for both rhythms, as compared to the 5-min Baseline period, during the early stage (first two minutes) of both restricted (Fig. 2E–J) and free (Fig. 2K–P) social interactions (paired t-test; Restricted interaction – rats: theta – t = −1.831, df = 15, p = 0.0435; gamma – t = 4.451, df = 15, p < 0.001; mice: theta – t = 5.3574, df = 24, p < 0.001; gamma – t = 9.8632, df = 24, p < 0.001; Free interaction – rats: theta – t = 3.980, df = 15, p < 0.001; gamma – t = 10.332, df = 15, p < 0.001; Restricted interaction – mice: theta – t = 3.1461, df = 25, p = 0.004; gamma – t = 8.3453, df = 25, p < 0.001). However, while the increase in theta rhythmicity was similar between rats and mice (Restricted interaction: independent t-test; t = 0.008, df = 40, p = 0.994; Free interaction: independent t-test; t = 1.154, df = 39, p = 0.255; Fig. 2G, M), the enhancement in gamma rhythmicity was significantly higher in rats than in mice for both types of social interaction (Restricted interaction: independent t-test; t = 2.809, df = 16.098, p = 0.013; Free interaction: independent t-test; t = 5.760, df = 20.242, p < 0.001; Fig. 2J, P). Gamma rhythmicity is thought to reflect coordinated neural activity in local networks (Buzsaki and Draguhn, 2004; Buzsaki and Wang, 2012; Uhlhaas et al., 2009). Therefore, the significantly stronger gamma rhythmicity in the MeA of rats suggests a generally higher level of neural activity in this area during the first minutes of encounter with a novel social stimulus in rats, as compared to mice.

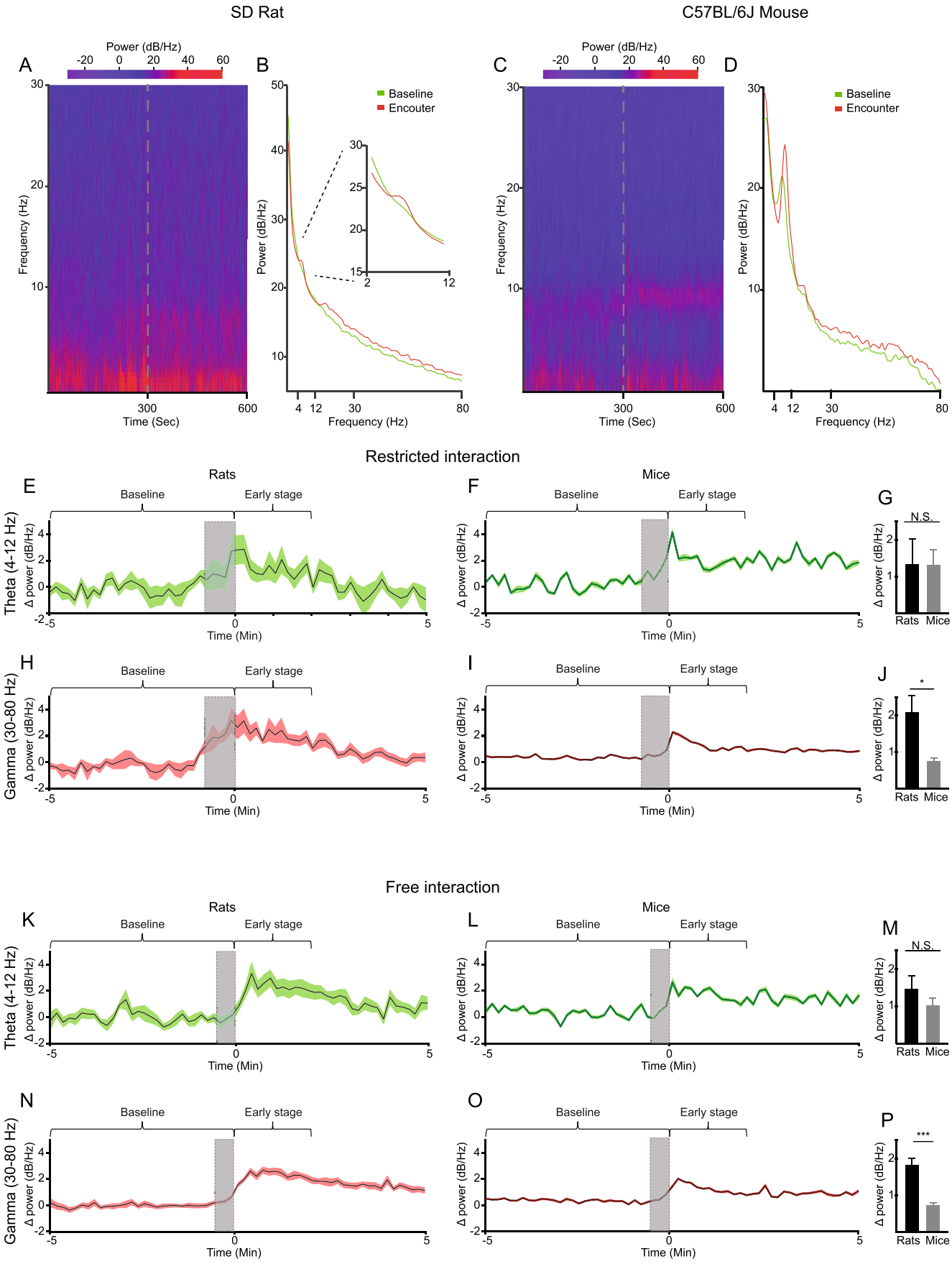
SD Rat
C57BL/6J Mouse
A
B
C
D
Power (dB/Hz)
-20 0 20 40 60
Frequency (Hz)
Time (Sec)
Power (dB/Hz)
Frequency (Hz)
Baseline
Encouter
Encounter
Restricted interaction
Rats
Mice
E
F
G
H
I
J
Baseline
Early stage
Theta (4-12 Hz)
Gamma (30-80 Hz)
Δ power (dB/Hz)
Time (Min)
N.S.
*
Rats
Mice
Free interaction
K
L
M
N
O
P
***

The increased theta and gamma rhythmicity during the social interaction may be induced by sensory inputs arriving during stimulus investigation bouts or reflect a general state induced by the social encounter. One way to tell between these possibilities is to examine whether the increased rhythmicity is locked to stimulus investigation bouts or not. Therefore, we analyzed the change in both theta and gamma rhythmicity during five seconds before and five seconds after the beginning of each investigation bout (marked by a dashed line in Fig. 3A–H). For normalizing the distinct bouts and sessions, we used *Z*-score analysis, with the 5-s pre-investigation period serving as a baseline. This analysis was conducted for restricted interaction sessions only, since investigation bouts are not well defined during free interactions. The heat-maps displayed in Fig. 3A–H show the *Z*-score of all bouts for each session, averaged separately for the social (Fig. 3A–D) and object (Fig. 3E–H) stimuli. As apparent from the mean traces shown in Fig. 3I–L, rats exhibited no significant bout-associated change in theta rhythmicity, for both social and object investigation (Fig. 3I, paired *t*-test; social – $t = 0.800$, df = 15, $p = 0.870$; object – $t = -0.8544$, df = 15, $p = 0.814$, with Bonferroni's correction for multiple comparisons). Gamma rhythmicity, on the other hand, showed small but significant increase during investigation bouts towards the social, but not to the object stimulus (Fig. 3K, paired *t*-test; social – $t = -2.499$, df = 15, $p = 0.048$; object – $t = -1.233$, df = 15, $p = 0.474$, with Bonferroni's correction for multiple comparisons). In contrast to rats, mice showed a clear induction of both theta and gamma rhythmicity immediately after the beginning of the social, but not object investigation bouts (Fig. 3J, L; paired *t*-test; Theta: social – $t = -3.627$, df = 24, $p = 0.002$; object – $t = 1.059$, df = 24, $p = 0.599$; Gamma: social – $t = -3.360$, df = 24, $p = 0.005$; object – $t = 1.020$, df = 24, $p = 0.634$, with Bonferroni's correction for multiple comparisons).

The difference between rats and mice is also supported by direct statistical comparison between them (Fig. 3M, N; Mixed-model ANOVA, Theta: species – $F_{1,77} = 3.036$, $p = 0.0854$; stimulus – $F_{1,77} = 2.322$, $p = 0.1316$; species × stimulus – $F_{1,77} = 9.488$, $p = 0.003$; Gamma: species – $F_{1,77} = 2.197$, $p = 0.1424$; stimulus – $F_{1,77} = 1.035$, $p = 0.3121$; species × stimulus – $F_{1,77} = 8.069$, $p = 0.006$).

Thus, we conclude that during social interaction with a novel same-sex conspecific, both theta and gamma rhythmicity in the MeA reflect distinct features in rats and mice. While in rats they reflect mainly a state in this brain area but do not change much during stimulus investigation bouts, in mice they are also associated with active events of social investigation.

DISCUSSION

Theta and gamma rhythms of LFP signals are well known from many brain areas, including the amygdala, and were associated with various cognitive and emotional behaviors (Bocchio et al., 2017; Buzsaki and Watson, 2012; Headley and Pare, 2013; Schonfeld and Wojtecki, 2019; Symons et al., 2016). Both are thought to reflect synchrony between neuronal populations (Buzsaki and Draguhn, 2004; Uhlhaas et al., 2009). Yet, while theta rhythmicity is assumed to represent synchrony between neuronal populations distributed between distinct, sometimes remote brain regions (Colgin, 2011; Gordon, 2011; Harris and Gordon, 2015), gamma rhythmicity is considered to reflect synchrony of local networks (Buzsaki and Wang, 2012; Headley and Pare, 2013). Accordingly, theta rhythmicity is considered as a top-down process, associated with extended brain states, such as arousal and attention, which are regulated by brain wide-active neuromodulators and engulf distributed brain networks (Clayton et al., 2015; Fiebelkorn and Kastner, 2019; Helfrich et al., 2019; Karakas, 2020; Knyazev, 2007). In contrast, gamma rhythmicity in various brain regions is considered as a bottom-up process, associated with specific inputs arriving to the local network (Benchenane et al., 2011; Buzsaki and Wang, 2012; Headley and Pare, 2013; Palva and Palva, 2018).

In a previous study (Tendler and Wagner, 2015), we revealed that free interaction between adult male SD rats is characterized by increased theta rhythmicity in multiple limbic brain regions, including the MeA, and that this increase is negatively correlated with the degree of familiarity between the interacting animals. Therefore, we concluded that theta rhythmicity in the MeA of SD rats reflects the level of arousal of the subject, which is proportional to

Fig. 2. Higher levels of session-wide gamma rhythmicity during social interaction in rats than in mice. (**A**) An example spectrogram (0–30 Hz) of LFP signals recorded from a rat subject across the 5-min Baseline and 5-min Encounter periods, separated by the dashed line. (**B**) Power spectral density (PSD) profiles (0–80 Hz) of the Baseline (green) and Encounter (red) periods shown in **(A)**. The inset displays the theta range at a higher resolution. Note the enhanced power of both theta (~8 Hz) and gamma (30–80 Hz) during encounter. (**C**) As in **(A)**, for a C57BL/6J mouse subject. (**D**) As in **(B)**, for the mouse recording shown in **(C)**. (**E**) Mean (± SEM) change in theta power (Δpower) from Baseline, across the Baseline and Encounter periods of restricted interaction of SD rats. Grey bar represents an estimation of the time used for stimuli delivery into the arena, while time 0 represents the beginning of the Encounter period. Note the increased power during the first minutes (Early stage) of the Encounter period. The Baseline and Early stage periods used for calculating the response are denoted above the trace. (**F**) As in **(E)**, for C57BL/6J mice. (**G**) A comparison of the mean Δpower of theta rhythmicity averaged across the first 2 min of the encounter (Early stage period), between rats and mice. **(H–J)** As in **(E–G)**, for gamma rhythmicity. Note the significantly higher level of induced gamma rhythmicity observed in rats, as compared to mice **(G)**. *$p < 0.05$, 2-tailed *t*-test. **(K–P)** As in **(E–J)**, for free interaction. The grey bar is shorter than in restricted interaction, as it takes less time to introduce a single stimulus to the arena. Time 0 represents the beginning of the Encounter period. Note the high similarity between the results obtained for restricted interaction **(E–J)** and those obtained for free interaction **(K–P)**. ***$p < 0.001$, 2-tailed *t*-test. (For interpretation of the references to colour in this figure legend, the reader is referred to the web version of this article.)

the novelty of the encountered conspecific. Furthermore, we showed that a distinct arousing setting of conditioned fear induced a different profile of theta rhythmicity than social interaction, in the same brain regions. These results suggest that theta rhythmicity in these regions of the rat brain is affective state-dependent (Tendler and Wagner, 2015). Our results here repeat these results and recapitulate them in a new setting of restricted social interaction. Moreover, by analyzing the temporal changes in theta rhythmicity relative to social investigation bouts,

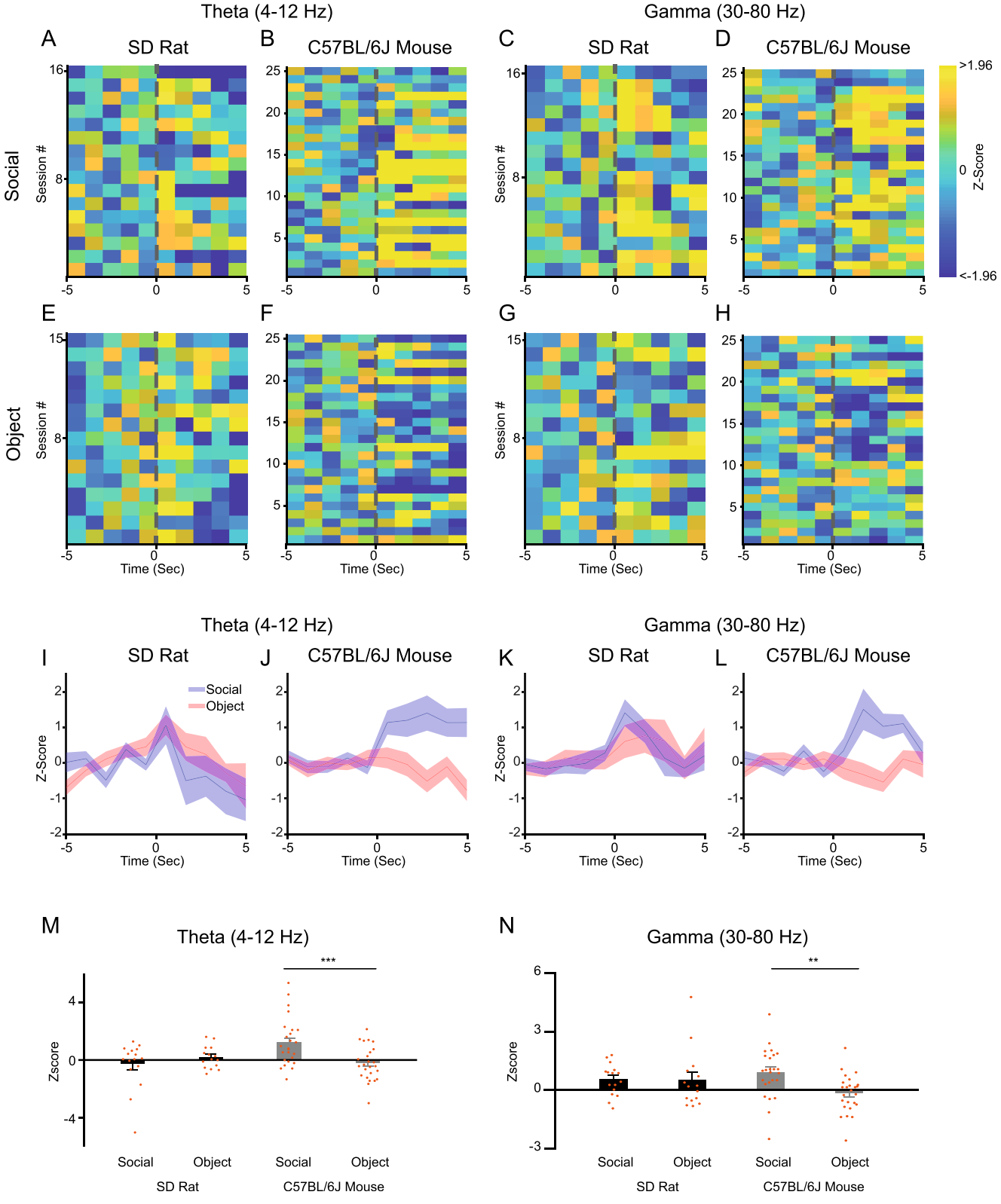

as enabled during restricted interaction, we demonstrated that most of these changes are not synchronized with stimulus investigation bouts. Even for gamma rhythmicity which was found to be significantly increased during social investigation bouts in rats, the bout-associated increase was small and its statistical significance was marginal. Given our observation that the change in gamma rhythmicity along the social interaction was twice as big in rats that in mice (Fig. 2J, P) while the social investigation bout-associated change in gamma rhythmicity was rather similar between them (Fig. 3K-L), it seems highly likely that most of the gamma rhythmicity change during social interaction in rats is driven by the behavioral state rather than by sensory inputs. Altogether, these results further support our previous interpretation that theta rhythmicity in the MeA, and most likely in other limbic brain regions of SD rats, reflect a state of motivation or arousal driven by the novelty and valance of the stimulus, more than processing of stimulus-specific information. Interestingly, gamma rhythmicity recorded by us in rats showed similar dynamics as theta rhythmicity, with significant general enhancement during the social interaction but very little correlation with social investigation bouts. Thus, gamma rhythmicity in the MeA of SD rats may also be associated with the brain state of the animal more than with specific inputs.

In contrast to rats, mice exhibited significant induction of both theta and gamma power in the first few seconds of social, but not object investigation bouts, suggesting that both rhythms are associated with sensory input arrival rather than an extended state. These results are in accordance with a previous study, where LFP signals were recorded from the olfactory bulb and MeA of freely behaving adult female mice while these animals were exposed to various social and non-social olfactory stimuli (Pardo-Bellver et al., 2017). In this study, the researchers revealed induction of both theta and gamma rhythmicity in synchronization with exploratory bouts towards the social cues, as we did here. Therefore, both theta and gamma rhythmicity in the murine MeA seem to be mostly associated with stimulus investigation, hence with arrival of sensory inputs.

Altogether, our results suggest that during social interaction with a novel same-sex conspecific, the balance between the two functions of the MeA differs between rats and mice. While in rats the function of the MeA as a state-dependent behavioral modulator dominates, the murine MeA seems to be more strongly involved in sensory information processing. The significant role of sensory information processing in the MeA of mice was demonstrated by multiple studies which recorded MeA neuronal responses to various specific social stimuli in mice (Bergan et al., 2014; Chen et al., 2019; Hu et al., 2021; Li et al., 2017; Yao et al., 2017b). Such recordings, however, are almost absent in rats.

It should be noted, that there is no doubt that the MeA is activated during interactions between male rats, as proved by multiple c-Fos expression studies by us (Netser et al., 2020) and others (for example, Weathington et al., 2012; Zhang et al., 2022). The results of such studies, however, cannot tell between MeA activation due to a motivational state and its excitation due to arrival of specific sensory inputs. This is because of the low temporal resolution of c-Fos expression, that integrates neuronal activity across several minutes. Similarly, multiple studies that demonstrated the importance of the rat MeA for social interactions by manipulating its activity (for example, Rasia-Filho et al., 2012b; Sano et al., 2016; Spiteri et al., 2010) cannot tell between state-dependent and sensory-input dependent activity. In order to discriminate between these two possibilities, one needs to record neuronal activity in behaving animals and to examine whether the MeA neuronal activity in locked to stimulus investigation or not, as we did here. Future studies using single-cell recordings in the MeA of behaving rats should examine if neuronal activity in this area indeed principally differ than what is reported in mice.

It should also be noted, that our results are limited to a specific behavioral context of male social interaction with a novel same-sex conspecific. It is therefore possible that in other contexts, such as mating, aggressive or parental behavior, sensory information processing may prevail in the MeA even in rats. For example, Multi-site recordings from the amygdala of anesthetized rats showed that the highest percentage of neuronal responses to cat urine of all recorded amygdaloid nuclei were obtained in the MeA (Govic and Paolini, 2015). Moreover, since the MeA is known to be a sexually-dimorphic brain area (Jennings and de Lecea, 2020), with a strong influence of steroid hormones over its neuronal network structure and plasticity (Rasia-Filho et al., 2012a), it might have a distinct mode of action in female rats.

In conclusion, our results suggest a distinct mode of action of the MeA during social interaction with a novel conspecific, between SD rats and C57BL/6J mice; While in C57BL/6J mice the MeA is mostly involved in sensory information processing, in SD rats it is mainly active in modulating the social motivation state of the animal.

Fig. 3. Increased theta and gamma power during social investigation bouts of mice but not rats. (**A**) Heat-maps of mean theta power before and during social investigation bouts of SD rats. Each line represents the mean *Z*-score of all bouts in a single session. Dashed line (Time 0) represents the beginning of the bout. (**B**) As in **(A)**, for C57BL6J mice. Note the clearly increased signal immediately after the beginning of the bout. **(C–D)** As in **(A–B)**, for gamma rhythmicity during social investigation bouts. **(E–H)** As in **(A–D)**, for object investigation bouts. (**I**) Mean (±SEM) *Z*-score of theta rhythmicity before and during rat social and object investigation bouts. Time 0 represents the beginning of the investigation bout. Note the similarity between the traces, demonstrating no difference in induction of theta power between the stimuli. (**J**) As in **(I)**, for mice. Note the clearly increased theta power during social investigation bouts, as compared to object investigation bouts. **(K–L)** As in **(I–J)**, for gamma rhythmicity. (**M**) A comparison of the mean change in theta power *Z*-score during 5 s following bout beginning, as compared to baseline, between stimuli for each of the species. ***$p < 0.001$, Holm–Sidak's *post hoc* test following main effect in a mixed-model ANOVA test. (**N**) As in **(L)**, for gamma rhythmicity. **$p < 0.01$, Holm–Sidak's *post hoc* test following main effect in a mixed-model ANOVA test.

CRediT authorship contribution statement

Shanah Rachel John: Investigation, Writing – original draft. **Wael Dagash:** Investigation. **Alok Nath Mohapatra:** Investigation, Writing – original draft, Visualization. **Shai Netser:** Conceptualization, Methodology, Software, Validation, Formal analysis, Data curation, Writing – original draft, Visualization, Project administration. **Shlomo Wagner:** Conceptualization, Validation, Resources, Writing – original draft, Supervision, Funding acquisition.

ACKNOWLEDGEMENTS

This study was supported by ISF-NSFC joint research program (grant No. 3459/20 to SW), the Israel Science Foundation (ISF grant 1361/17 to SW), the Ministry of Science, Technology and Space of Israel (Grant No. 3-12068 to SW) and the United States-Israel Binational Science Foundation (BSF grant No. 2019186 to SW).

INSTITUTIONAL REVIEW BOARD STATEMENT

All experiments were performed according to the National Institutes of Health guide for the care and use of laboratory animals and approved by the Institutional Animal Care and Use Committee (IACUC) of the University of Haifa.

CONFLICTS OF INTEREST

The authors declare no conflict of interest.

DATA AVAILABILITY

All data used for this study are deposited in Mendeley Data using the following reference – ‘‘Raw data for paper – Distinct dynamics of theta and gamma rhythmicity during social interaction suggest differential mode of action in the medial amygdala of SD rats and C57BL/6J mice”, Mendeley Data, V2, doi: 10.17632/fgsw49mc9k.2.

REFERENCES

Allsop SA, Wichmann R, Mills F, Burgos-Robles A, Chang C-J, Felix-Ortiz AC, Vienne A, Beyeler A, Izadmehr EM, Glober G, Cum MI, Stergiadou J, Anandalingam KK, Farris K, Namburi P, Leppla CA, Weddington JC, Nieh EH, Smith AC, Ba D, Brown EN, Tye KM (2018) Corticoamygdala transfer of socially derived information gates observational learning. Cell 173:1329.

Amadei EA, Johnson ZV, Jun Kwon Y, Shpiner AC, Saravanan V, Mays WD, Ryan SJ, Walum H, Rainnie DG, Young LJ, Liu RC (2017) Dynamic corticostriatal activity biases social bonding in monogamous female prairie voles. Nature 546:297–301.

Arakawa H, Arakawa K, Deak T (2010) Oxytocin and vasopressin in the medial amygdala differentially modulate approach and avoidance behavior toward illness-related social odor. Neuroscience 171:1141–1151.

Argue KJ, VanRyzin JW, Falvo DJ, Whitaker AR, Yu SJ, McCarthy MM (2017) Activation of both CB1 and CB2 endocannabinoid receptors is critical for masculinization of the developing medial amygdala and juvenile social play behavior. Eneuro 4.

S. Atzil A. Touroutoglou T. Rudy S. Salcedo R. Feldman J.M. Hooker B.C. Dickerson C. Catana L.F. Barrett Dopamine in the medial amygdala network mediates human bonding Proc Natl Acad Sci U S A 114 9 2017 2361 2366.

Benchenane K, Tiesinga PH, Battaglia FP (2011) Oscillations in the prefrontal cortex: a gateway to memory and attention. Curr Opin Neurobiol 21:475–485.

Bergan JF, Ben-Shaul Y, Dulac C (2014) Sex-specific processing of social cues in the medial amygdala. Elife 3.

Bocchio M, Nabavi S, Capogna M (2017) Synaptic plasticity, engrams, and network oscillations in amygdala circuits for storage and retrieval of emotional memories. Neuron 94:731–743.

Buzsaki G, Draguhn A (2004) Neuronal oscillations in cortical networks. Science 304:1926–1929.

Buzsaki G, Wang X-J (2012) Mechanisms of gamma oscillations. Annu Rev Neurosci 35:203–225.

Buzsaki G, Watson BO (2012) Brain rhythms and neural syntax: implications for efficient coding of cognitive content and neuropsychiatric disease. Dialogues Clin Neurosci 14:345–367.

Cannon J, McCarthy MM, Lee S, Lee J, Börgers C, Whittington MA, Kopell N (2014) Neurosystems: brain rhythms and cognitive processing. Eur J Neurosci 39:705–719.

Chen PB, Hu RK, Wu YE, Pan L, Huang S, Micevych PE, Hong W (2019) Sexually dimorphic control of parenting behavior by the medial amygdala. Cell 176, 1206-1221 e1218.

Clayton MS, Yeung N, Cohen Kadosh R (2015) The roles of cortical oscillations in sustained attention. Trends Cogn Sci 19:188–195.

Colgin LL (2011) Oscillations and hippocampal-prefrontal synchrony. Curr Opin Neurobiol 21:467–474.

Cushing BS, Perry A, Musatov S, Ogawa S, Papademetriou E (2008) Estrogen receptors in the medial amygdala inhibit the expression of male prosocial behavior. J Neurosci 28:10399–10403.

Dolen G, Darvishzadeh A, Huang KW, Malenka RC (2013) Social reward requires coordinated activity of nucleus accumbens oxytocin and serotonin. Nature 501:179–184.

Dulac C, Wagner S (2006) Genetic analysis of brain circuits underlying pheromone signaling. Annu Rev Genet 40(1): 449–467.

Dumais KM, Alonso AG, Bredewold R, Veenema AH (2016) Role of the oxytocin system in amygdala subregions in the regulation of social interest in male and female rats. Neuroscience 330:138–149.

Fiebelkorn IC, Kastner S (2019) A rhythmic theory of attention. Trends Cogn Sci 23:87–101.

Frankiensztajn LM, Gur-Pollack R, Wagner S (2018) A combinatorial modulation of synaptic plasticity in the rat medial amygdala by oxytocin, urocortin3 and estrogen. Psychoneuroendocrinology 92:95–102.

Fujisawa S, Buzsaki G (2011) A 4 Hz oscillation adaptively synchronizes prefrontal, VTA, and hippocampal activities. Neuron 72:153–165.

Gadziola MA, Grimsley JMS, Shanbhag SJ, Wenstrup JJ (2012) A novel coding mechanism for social vocalizations in the lateral amygdala. J Neurophysiol 107:1047–1057.

Gangopadhyay P, Chawla M, Dal Monte O, Chang SWC (2021) Prefrontal-amygdala circuits in social decision-making. Nat Neurosci 24:5–18.

Gordon JA (2011) Oscillations and hippocampal-prefrontal synchrony. Curr Opin Neurobiol 21:486–491.

Govic A, Paolini AG (2015) In vivo electrophysiological recordings in amygdala subnuclei reveal selective and distinct responses to a behaviorally identified predator odor. Journal of Neurophysiology 113:1423–1436.

Haller J (2018) The role of central and medial amygdala in normal and abnormal aggression: A review of classical approaches. Neurosci Biobehav Rev 85:34–43.

Harris AZ, Gordon JA (2015) Long-range neural synchrony in behavior. Annu Rev Neurosci 38:171–194.

Headley DB, Pare D (2013) In sync: gamma oscillations and emotional memory. Front Behav Neurosci 7:170.
Helfrich RF, Breska A, Knight RT (2019) Neural entrainment and network resonance in support of top-down guided attention. Curr Opin Psychol 29:82–89.
Hu RK, Zuo Y, Ly T, Wang J, Meera P, Wu YE, Hong W (2021) An amygdala-to-hypothalamus circuit for social reward. Nat Neurosci 24:831–842.
Huang W-C, Zucca A, Levy J, Page DT (2020) Social behavior is modulated by valence-encoding mPFC-amygdala sub-circuitry. Cell Rep 32:107899.
Jennings KJ, de Lecea L (2020) Neural and hormonal control of sexual behavior. Endocrinology 161.
Jutras MJ, Buffalo EA (2010) Synchronous neural activity and memory formation. Curr Opin Neurobiol 20:150–155.
Karakas S (2020) A review of theta oscillation and its functional correlates. Int J Psychophysiol 157:82–99.
Knyazev GG (2007) Motivation, emotion, and their inhibitory control mirrored in brain oscillations. Neurosci Biobehav R 31:377–395.
Kohl J, Autry AE, Dulac C (2017) The neurobiology of parenting: A neural circuit perspective. Bioessays 39:1–11.
Kwon J-T, Ryu C, Lee H, Sheffield A, Fan J, Cho DH, Bigler S, Sullivan HA, Choe HK, Wickersham IR, Heiman M, Choi GB (2021) An amygdala circuit that suppresses social engagement. Nature 593:114–118.
LeDoux J (2007) The amygdala. Curr Biol 17:R868–R874.
Li D, Zhou C (2011) Organization of anti-phase synchronization pattern in neural networks: what are the key factors? Front Syst Neurosci 5:100.
Li Y, Mathis A, Grewe BF, Osterhout JA, Ahanonu B, Schnitzer MJ, Murthy VN, Dulac C (2017) Neuronal representation of social information in the medial amygdala of awake behaving mice. Cell 171(5):1176.
Lisman J (2005) The theta/gamma discrete phase code occurring during the hippocampal phase precession may be a more general brain coding scheme. Hippocampus 15:913–922.
Martinez-Marcos A (2009) On the organization of olfactory and vomeronasal cortices. Prog Neurobiol 87:21–30.
Mucignat-Caretta C (2010) The rodent accessory olfactory system. J Comp Physiol A Neuroethol Sens Neural Behav Physiol 196:767–777.
Netser S, Haskal S, Magalnik H, Bizer A, Wagner S (2019) A system for tracking the dynamics of social preference behavior in small rodents. J Vis Exp.
Netser S, Meyer A, Magalnik H, Zylbertal A, de la Zerda SH, Briller M, Bizer A, Grinevich V, Wagner S (2020) Distinct dynamics of social motivation drive differential social behavior in laboratory rat and mouse strains. Nat Commun 11:5908.
Newman SW (1999) The medial extended amygdala in male reproductive behavior. A node in the mammalian social behavior network. Ann N Y Acad Sci 877:242–257.
Opendak M, Raineki C, Perry RE, Rincon-Cortes M, Song SC, Zanca RM, Wood E, Packard K, Hu S, Woo J, *et al.* (2021) Bidirectional control of infant rat social behavior via dopaminergic innervation of the basolateral amygdala. Neuron 109, 4018-4035 e4017.
Palva JM, Palva S (2018) Functional integration across oscillation frequencies by cross-frequency phase synchronization. Eur J Neurosci 48:2399–2406.
Pardo-Bellver C, Martinez-Bellver S, Martinez-Garcia F, Lanuza E, Teruel-Marti V (2017) Synchronized activity in the main and accessory olfactory bulbs and vomeronasal amygdala elicited by chemical signals in freely behaving mice. Sci Rep 7:9924.
Park G, Ryu C, Kim S, Jeong SJ, Koo JW, Lee Y-S, Kim SJ (2021) Social isolation impairs the prefrontal-nucleus accumbens circuit subserving social recognition in mice. Cell Rep 35.
Petrulis A (2013) Chemosignals and hormones in the neural control of mammalian sexual behavior. Front Neuroendocrinol 34:255–267.
Raam T, Hong W (2021) Organization of neural circuits underlying social behavior: A consideration of the medial amygdala. Curr Opin Neurobiol 68:124–136.
Rasia-Filho AA, Dalpian F, Menezes IC, Brusco J, Moreira JE, Cohen RS (2012a) Dendritic spines of the medial amygdala: plasticity, density, shape, and subcellular modulation by sex steroids. Histol Histopathol 27:985–1011.
Rasia-Filho AA, Haas D, de Oliveira AP, de Castilhos J, Frey R, Stein D, Lazzari VM, Back F, Pires GN, Pavesi E, et al. (2012b) Morphological and functional features of the sex steroid-responsive posterodorsal medial amygdala of adult rats. Mini Rev Med Chem 12:1090–1106.
Sah P, Faber ESL, Lopez de armentia M, Power J (2003) The amygdaloid complex: anatomy and physiology. Physiol Rev 83:803–834.
Sano K, Nakata M, Musatov S, Morishita M, Sakamoto T, Tsukahara S, Ogawa S (2016) Pubertal activation of estrogen receptor alpha in the medial amygdala is essential for the full expression of male social behavior in mice. Proc Natl Acad Sci U S A 113:7632–7637.
Schonfeld LM, Wojtecki L (2019) Beyond emotions: oscillations of the amygdala and their implications for electrical neuromodulation. Front Neurosci-Switz 13.
Shemesh Y, Forkosh O, Mahn M, Anpilov S, Sztainberg Y, Manashirov S, Shlapobersky T, Elliott E, Tabouy L, Ezra G, Adler ES, Ben-Efraim YJ, Gil S, Kuperman Y, Haramati S, Dine J, Eder M, Deussing JM, Schneidman E, Yizhar O, Chen A (2016) Ucn3 and CRF-R2 in the medial amygdala regulate complex social dynamics. Nat Neurosci 19:1489–1496.
Spiteri T, Musatov S, Ogawa S, Ribeiro A, Pfaff DW, Agmo A (2010) The role of the estrogen receptor alpha in the medial amygdala and ventromedial nucleus of the hypothalamus in social recognition, anxiety and aggression. Behav Brain Res 210:211–220.
Stephens SBZ, Kauffman AS (2017) Regulation and possible functions of kisspeptin in the medial amygdala. Front Endocrinol (Lausanne) 8:191.
Symons AE, El-Deredy W, Schwartze M, Kotz SA (2016) The functional role of neural oscillations in non-verbal emotional communication. Front Hum Neurosci 10.
A. Tendler S. Wagner Different types of theta rhythmicity are induced by social and fearful stimuli in a network associated with social memory Elife 4 2015.
Twining RC, Vantrease JE, Love S, Padival M, Rosenkranz JA (2017) An intra-amygdala circuit specifically regulates social fear learning. Nat Neurosci 20:459–469.
Uhlhaas PJ, Pipa G, Lima B, Melloni L, Neuenschwander S, Nikolic D, Singer W (2009) Neural synchrony in cortical networks: history, concept and current status. Front Integr Neurosci 3:17.
Unger E, Burke K, Yang C, Bender K, Fuller P, Shah N (2015) Medial amygdalar aromatase neurons regulate aggression in both sexes. Cell Rep 10:453–462.
van Kerkhof LW, Trezza V, Mulder T, Gao P, Voorn P, Vanderschuren LJ (2014) Cellular activation in limbic brain systems during social play behaviour in rats. Brain Struct Funct 219:1181–1211.
Walsh JJ, Christoffel DJ, Heifets BD, Ben-Dor GA, Selimbeyoglu A, Hung LW, Deisseroth K, Malenka RC (2018) 5-HT release in nucleus accumbens rescues social deficits in mouse autism model. Nature 560:589–594.
Walum H, Young LJ (2018) The neural mechanisms and circuitry of the pair bond. Nat Rev Neurosci 19:643–654.
Wang XJ (2010) Neurophysiological and computational principles of cortical rhythms in cognition. Physiol Rev 90:1195–1268.
Weathington JM, Strahan JA, Cooke BM (2012) Social experience induces sex-specific fos expression in the amygdala of the juvenile rat. Horm Behav 62:154–161.
Williams AV, Duque-Wilckens N, Ramos-Maciel S, Campi KL, Bhela SK, Xu CK, Jackson K, Chini B, Pesavento PA, Trainor BC (2020)

Social approach and social vigilance are differentially regulated by oxytocin receptors in the nucleus accumbens. Neuropsychopharmacology 45:1423–1430.
Yao S, Bergan J, Lanjuin A, Dulac C (2017) Oxytocin signaling in the medial amygdala is required for sex discrimination of social cues. Elife 6.
Zhang X, Kiyokawa Y, Takeuchi Y (2022) Mapping of c-Fos expression in the medial amygdala following social buffering in male rats. Behav Brain Res 422.

APPENDIX A. SUPPLEMENTARY DATA

Supplementary data to this article can be found online at https://doi.org/10.1016/j.neuroscience.2022.04.020.

(Received 23 January 2022, Accepted 22 April 2022)
(Available online 28 April 2022)